Rational design and characterization of a Rac GTPase-specific small molecule inhibitor

Yuan Gao*, J. Bradley Dickerson†, Fukun Guo*, Jie Zheng†, and Yi Zheng*‡

*Division of Experimental Hematology, Children's Hospital Research Foundation, Cincinnati, OH 45229; and †Department of Structure Biology, St. Jude Children's Research Hospital, Memphis, TN 38105

Edited by Lewis C. Cantley, Harvard Institutes of Medicine, Boston, MA, and approved March 30, 2004 (received for review November 13, 2003)

The signaling pathways mediated by Rho family GTPases have been implicated in many aspects of cell biology. The specificity of the pathways is achieved in part by the selective interaction between Dbl family guanine nucleotide exchange factors (GEFs) and their Rho GTPase substrates. Here, we report a first-generation small-molecule inhibitor of Rac GTPase targeting Rac activation by GEF. The chemical compound NSC23766 was identified by a structure-based virtual screening of compounds that fit into a surface groove of Rac1 known to be critical for GEF specification. *In vitro* it could effectively inhibit Rac1 binding and activation by the Rac-specific GEF Trio or Tiam1 in a dose-dependent manner without interfering with the closely related Cdc42 or RhoA binding or activation by their respective GEFs or with Rac1 interaction with BcrGAP or effector PAK1. In cells, it potently blocked serum or platelet-derived growth factor-induced Rac1 activation and lamellipodia formation without affecting the activity of endogenous Cdc42 or RhoA. Moreover, this compound reduced Trio or Tiam1 but not Vav, Lbc, Intersectin, or a constitutively active Rac1 mutant-stimulated cell growth and suppressed Trio, Tiam1, or Ras-induced cell transformation. When applied to human prostate cancer PC-3 cells, it was able to inhibit the proliferation, anchorage-independent growth and invasion phenotypes that require the endogenous Rac1 activity. Thus, NSC23766 constitutes a Rac-specific small-molecule inhibitor that could be useful to study the role of Rac in various cellular functions and to reverse tumor cell phenotypes associated with Rac deregulation.

Rho family GTPases are molecular switches that control signaling pathways regulating cytoskeleton organization, gene expression, cell cycle progression, cell motility, and other cellular processes (1). They can be activated through the interaction with the Dbl family guanine nucleotide exchange factors (GEFs) that catalyze their GTP/GDP exchange and connect them to the diverse stimuli from upstream cell surface receptors such as the G protein-coupled receptors, growth factor receptors, cytokine receptors, and adhesion receptors (2). Accumulating evidence has implicated Rho GTPases in many aspects of cancer development (3–6), and deregulated Rho GTPases have been discovered in many human tumors, including colon, breast, lung, myeloma, and head and neck squamous-cell carcinoma (7–11). Rho GTPases and the signal pathways regulated by them have thus been proposed as potential anticancer therapeutic targets (12). Because in many cases it is overexpression or up-regulation, not constitutively activating mutation, of individual Rho protein that is associated with tumorigenic properties or poor prognosis of cancer, one targeting strategy of a Rho GTPase signal pathway may come by inhibition of the Rho GTPase activation by its specific Dbl family GEF.

Because the number of the Dbl family GEFs appears to far outnumber that of Rho GTPase substrates (2), the signaling specificity mediated by Rho proteins is in part governed by specific GEF–Rho interactions. Recently available 3D structures of GEF–Rho protein complexes provided a wealth of information on the mechanism of GEF–Rho GTPase interactions (13–15). In the previous structural mapping studies of Rac1 interaction with its GEFs, we and others have identified a groove formed by the switch I, switch II, and $\beta1/\beta2/\beta3$ regions of Rac1 as the key area involved in GEF specification and pinpointed residue Trp^{56} as the critical determinant of Rac1 for discrimination by a subset of Rac1-specific GEFs including Trio and Tiam1 (16). The Rac1 mutant Rac1W56F lost its responsiveness and the ability to interact with Trio and Tiam1, whereas the corresponding Cdc42 mutant Cdc42F56W gained the sensitivity to Trio and Tiam1 (16, 17). Moreover, we have shown that a polypeptide derived from Rac1 sequences containing Trp^{56} can specifically inhibit GEF binding to Rac1 (16), raising the possibility that the structural features surrounding Trp^{56} of Rac1 might be explored for the design of an interfering reagent specifically blocking Rac1 activation by its GEF.

In the present work, we have applied a structure-based virtual screening approach (18) to the search for a Rac–GEF interaction-specific small-molecule inhibitor. By screening the chemical library of National Cancer Institute we have identified a chemical compound, NSC23766, that fits well into the GEF-recognition groove centering on Trp^{56} of Rac1. We show that NSC23766 acts as a Rac activation-specific inhibitor that could be useful for cell biological studies of Rac function and for therapeutic targeting at Rac deregulation.

Experimental Procedures

Virtual Screening. The UNITY program (Tripos Associates, St. Louis) was used to screen the National Cancer Institute database for chemical compounds that were able to fit into the Rac1 surface containing Trp^{56}. The candidate compounds were then docked onto the Rac1 surface by using the program FLEXX (Tripos Associates) for energy minimization (19). The chemical compounds displaying the highest binding affinities in the calculations were obtained from the Drug Synthesis and Chemistry Branch, Developmental Therapeutics Program, Division of Cancer Treatment and Diagnosis, National Cancer Institute, for further experimental tests.

Recombinant Protein Production. See *Supporting Text*, which is published as supporting information on the PNAS web site.

***In Vitro* Complex Formation Assay.** About 0.5 μg of $(His)_6$-tagged TrioN was incubated with 0.5 μg of EDTA-treated, GST-fused Cdc42 or Rac1 in a binding buffer containing 20 mM Tris·HCl (pH 7.6), 100 mM NaCl, 1 mM DTT, 1% BSA, 1% Triton X-100, 1 mM $MgCl_2$, and 10 μl of suspended glutathione-agarose beads. GST-tagged Intersectin ($\approx$0.75 μg) was incubated with nucleotide-free, His-6-tagged Cdc42 or Rac1 (0.25 μg) in the binding buffer with 10 μl of suspended glutathione-agarose beads. Compound 23766 or other chemicals were added in the incubation buffer at the indicated concentrations. After incubation at 4°C for 30 min under constant agitation, the glutathione beads were washed twice with the binding buffer. The amount of $(His)_6$-tagged protein coprecipitated with the GST-fusion-bound beads was detected by anti-His Western blotting. Similarly, cell lysates containing myc-Tiam1, AU-PDZ-

This paper was submitted directly (Track II) to the PNAS office.

Abbreviations: GEF, guanine nucleotide exchange factor; PDGF, platelet-derived growth factor.

‡To whom correspondence should be addressed at: Division of Experimental Hematology, Children's Hospital Research Foundation, 3333 Burnet Avenue, Cincinnati, OH 45229. E-mail: yi.zheng@chmcc.org.

www.pnas.org/cgi/doi/10.1073/pnas.0307512101

RhoGEF, or $(His)_6$-Rac1 were mixed with purified $(His)_6$-Rac1, GST-RhoA, GST-BcrGAP, or GST-PAK1, and the pairwise association between the proteins was assessed in the presence of the indicated amount of 23766 in the respective assays.

***In Vitro* Guanine Nucleotide-Exchange Assay.** Assayed for their nucleotide-exchange activities in the absence or presence of 200 nM TrioN, Intersectin, or PDZ-RhoGEF, were 200 nM Rac1, Cdc42, or RhoA loaded with mant-GDP, as described (20).

Endogenous Rho GTPase Activity Assay. Cells were grown in log phase in a 10-cm dish, and were starved in 0.5% serum medium or indicated otherwise for 24 h before lysis in a buffer containing 20 mM Tris·HCl (pH 7.6), 100 mM NaCl, 10 mM $MgCl_2$, 1% Nonidet P-40, 10% glycerol, and 1× protease inhibitor mixture (Roche Molecular Biochemicals). Lysates were clarified, the protein concentrations were normalized, and the GTP-bound Rac1, Cdc42, or RhoA in the lysates were measured by an effector domain pull-down assay as described (16).

Immunofluorescence. See *Supporting Text*.

Cell Growth Assay. Wild-type, L61Rac1, or various GEF-transfected NIH 3T3 cells were grown in 5% calf serum. The cells were split in duplicate in six-well plates at 5×10^4 cells per well in the presence or absence of indicated amount of 23766 and were counted daily. The growth rate of the prostate PC-3 cells was measured by the CellTiter 96 AQueous assay (Promega); 1,500 cells per well in 200 μl of 5% FBS medium were plated in 96-well plates and were grown under normal conditions.

Anchorage-Independent Growth Assay. The Rac1, Ras, or Tiam1-transformed NIH 3T3 cells and prostate epithelia RWPE and PC-3 cells (1.25×10^3 per well) were grown in 0.3% agarose in the absence or presence of different doses of compound 23766 as described (21).

Cell Invasion Assay. Cell invasions were measured by using 6.4-mm Biocoat Matrigel invasion chambers with 8.0-μm pore size membrane (Becton Dickinson) as described (22).

Results

Virtual Screening for Rac-Specific Docking Compounds. In the 3D structure of the Rac1–Tiam1 complex, Trp^{56} of Rac1 is buried in a pocket formed by residues His^{1178}, $Ser1^{184}$, Glu^{1183}, and Ile^{1197} of Tiam1 and Lys^5, Val^7, Thr^{58}, and Ser^{71} of Rac1 (13). To identify Rac1-specific inhibitors based on the structural features surrounding Trp^{56}, a putative inhibitor-binding pocket was created with residues of Rac1 within 6.5 Å of Trp^{56} in the Rac1-Tiam1 monomer, including Lys^5, Val^7, Trp^{56}, and Ser^{71}. A 3D database search was performed to identify compounds whose conformations would fit into this pocket. The database we used was freely available from National Cancer Institute (www.dtp.nih.gov), which includes the coordinates of >140,000 small chemical compounds. To take the flexibility of the compounds into consideration during the screening process, the program UNITY, whose Directed Tweak algorithm allows a conformationally flexible 3D search (23), was applied. The small-molecule hits yielded by the UNITY program were next docked into the predicted binding pocket of Rac1 containing Trp^{56} by using the program FLEXX, an energy minimization modeling software that allows flexible docking to protein-binding sites (24). By following the docking procedures, the compounds were ranked based on their predicted ability to bind to the binding pocket with the program CSCORE. CSCORE generates a relative, consensus score based on how well the individual scoring functions of the protein–ligand complex perform (25). Of the top 100 compounds that displayed high consensus scores, we crossed out 58 compounds whose docking did not seem to involve residue Trp^{56} by visual inspection. Taking into account the solubility and availability of the remaining compounds, we focused on a set of 15 chemicals that show promising docking affinities by the scoring method for further characterization.

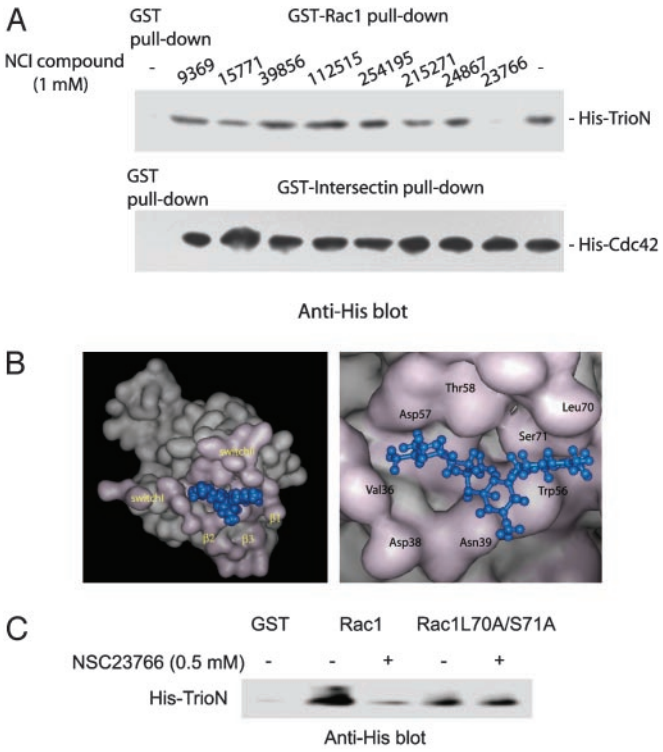

Fig. 1. Identification of NSC23766 as an inhibitor of Rac1–Trio interaction. (*A upper*) The inhibitory effect of a panel of compounds predicted by virtual screening on Rac1 interaction with TrioN was tested in a complex formation assay. $(His)_6$-tagged TrioN (0.5 μg) was incubated with GST alone or nucleotide-free GST-Rac1 (2 μg) in the presence or absence of 1 mM indicated National Cancer Institute compound and 10 μl of suspended glutathione-agarose beads. After an incubation at 4°C for 30 min, the beads associated $(His)_6$-TrioN were detected by anti-His Western blotting. (*A Lower*) The effect of the compounds on Cdc42 binding to Intersectin was determined similarly; ≈1 μg of GST or GST-tagged Intersectin was incubated with the nucleotide-free, $(His)_6$-tagged Cdc42 (0.25 μg) under similar conditions. Data are representative of the results from four independent experiments. (*B*) A simulated docking model of NSC23766 on Rac1 surface. The docking model was generated with the FLEXX program and was visualized with VIEWERPRO. (*Left*) A top view of the binding pocket of Rac1 bound to NSC23766. (*Right*) Predicted structural contacts of NSC23766 in the binding pocket of Trp^{56}. (*C*) The inhibitory effect of NSC23766 was examined with the Rac1L70A/S71A mutant binding to TrioN.

Compound 23766 Specifically Inhibited Rac1–GEF Interaction *in Vitro*. The 15 chemical compounds generated by virtual screening were examined for their ability to inhibit the Rac1-binding interaction with its GEF in a complex formation assay. For this purpose, TrioN, which specifically activates Rac1 but not Cdc42 (16) and Intersectin, a Cdc42-specific GEF (17), were used to assay the binding activity to their respective substrates in the presence of a 1-mM concentration of each individual compound. As shown in Fig. 1*A*, TrioN readily coprecipitated with GST-Rac1 but not with GST. Among the compounds tested, NSC23766 was the only one to significantly inhibit TrioN binding to Rac1. The inhibitory effect of NSC23766 appeared to be specific for the interaction between Rac1 and its GEF because it did not interfere with the Cdc42 binding to Intersectin.

The chemical structure of NSC23766 is shown in Fig. 7, which is published as supporting information on the PNAS web site. On examination of the docking model, it appears that the binding site for NSC23766 on Rac1 is a surface cleft formed by residues Lys^5,

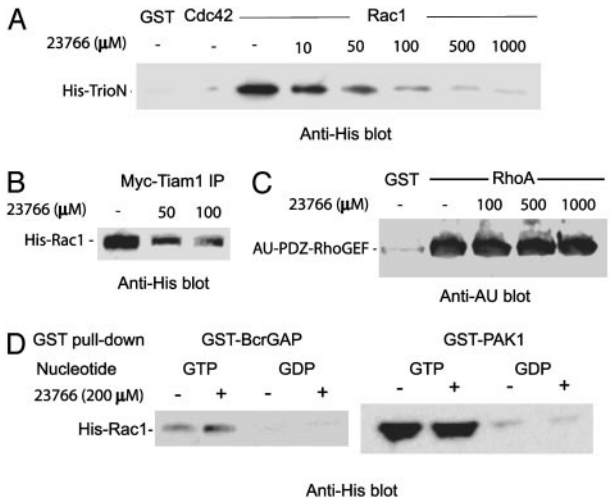

Fig. 2. Dose-dependent specific inhibition of GEF interaction with Rac1 by NSC23766. (*A*) $(His)_6$-tagged TrioN (0.5 μg) was incubated with GST alone or nucleotide-free, GST-fused Cdc42 or Rac1 (2 μg) in the binding buffer containing different concentrations of NSC23766 and 10 μl of suspended glutathione-agarose. The beads associated $(His)_6$-TrioN were detected by anti-His Western blotting. (*B*) myc-tagged Tiam1 expressed in Cos-7 cell lysates were incubated with $(His)_6$-Rac1 in the presence of increasing concentrations of NSC23766. The association of Rac1 with Tiam1 was examined by anti-His blotting after anti-myc immunoprecipitation. (*C*) The AU-tagged PDZ-RhoGEF was expressed in Cos-7 lysates and incubated with GST or GST-RhoA in the presence of varying concentrations of NSC23766. The RhoA-associated PDZ-RhoGEF was probed with anti-AU antibody after affinity precipitation by glutathione agarose beads. (*D*) $(His)_6$-Rac1 loaded with GDP or GTPγS was incubated with GST-BcrGAP or GST-PAK1 (p21-binding domain) in the presence or absence of 200 μM NSC23766, and the interaction with GST-BcrGAP or GST-PAK1 was probed by anti-His blot after affinity precipitation by glutathione agarose beads.

Asp^{38}, Asn^{39}, Trp^{56}, Asp^{57}, Thr^{58}, Leu^{70}, and Ser^{71} (Fig. 1*B*), conforming to the previously predicted groove among the switch I, switch II, and $\beta1/\beta2/\beta3$ regions that is the key area involved in GEF specification. Mutation of most residues in this region impaired GEF binding and/or catalysis. As shown in Fig. 1*C*, Rac1L70A/S71A retained binding to TrioN but lost the inhibitory response to NSC23766, suggesting that the chemical may indeed use the predicted docking pocket of Rac1 for the interference of GEF recognition.

Further examination of NSC23766 revealed that it can inhibit Rac1–TrioN interaction in a dose-dependent manner, achieving 50% inhibition at $\approx$50 μM under the GST pull-down conditions (Fig. 2*A* and Fig. 8, which is published as supporting information on the PNAS web site). Increasing the GEF dose in the pull-down assay could significantly hinder the inhibitory effect (data not shown), consistent with a competitive nature of the inhibitor action. To see whether the inhibitory activity of NSC23766 toward Rac–TrioN interaction could be extended to other Rac-specific GEF and whether the chemical interferes with the GEF interaction specifically, we next tested its effect on Rac1–Tiam1, RhoA–PDZ-RhoGEF, Rac1–BcrGAP, and Rac1–PAK1 interactions. As shown in Fig. 2 *B–D*, the compound inhibited Tiam1 binding to Rac1 similarly to TrioN but had no detectable effect on RhoA binding to its GEF or PDZ-RhoGEF or on Rac1 binding to BcrGAP or effector PAK1. These results suggest that NSC23766 is capable of specifically interfering with Rac1–GEF interaction.

To determine whether NSC23766 is active in specifically inhibiting GEF-stimulated guanine nucleotide-exchange reaction of Rac1, the mant-GDP/GTP exchange assays of Rac1, Cdc42, and RhoA under the catalysis of TrioN, Intersectin, and PDZ-RhoGEF, respectively, were carried out in the presence of increasing doses of NSC23766. As shown in Fig. 9, which is published as supporting information on the PNAS web site, the chemical was able to block the nucleotide exchange of Rac1 catalyzed by TrioN in a dose-dependent manner. The 50% inhibitory dose came at $\approx$50 μM, consistent with the inhibitory potency of the binding interaction (Fig. 2*A*). In contrast, the compound had little impact on the Intersectin-stimulated mant-GDP/GTP exchange of Cdc42 or on the PDZ-RhoGEF-stimulated mant-GDP/GTP exchange of RhoA at 200 μM concentration (Fig. 9). These results demonstrate that NSC23766 is able to specifically inhibit the activation of Rac1 by its GEF *in vitro*.

Specific Inhibitory Effect of NSC23766 on Rac1 Activity *in Vivo*. In fibroblasts, Rac1 can be activated by diverse stimuli, including serum and platelet-derived growth factor (PDGF) (26, 27), and this activation is expected to be mediated by one or more Rac-specific GEFs, such as Tiam1. To evaluate whether NSC23766 might affect Rac activity *in vivo*, NIH 3T3 cells grown in 10% calf serum were treated with NSC23766 in different concentrations overnight, and the activation state of endogenous Rac1 in the cells was detected by an effector domain pull-down assay. As shown in Fig. 3*A*, NSC23766 strongly inhibited Rac1 activation induced by serum, and the inhibitory effect of NSC23766 appeared to be specific toward Rac among Rho GTPases, because the activation states of Cdc42 and RhoA in the same cells were not affected by the presence of up to 100 μM NSC23766 (Fig. 3*A*). To examine whether NSC23766 can affect Rac1 activation by PDGF stimulation, serum-starved NIH 3T3 cells in the presence or absence of 50 or 100 μM compound were challenged with 10 nM PDGF for 2 min, and the cell lysates were assayed for the amount of active Rac1-GTP. Comparing with the Rac1 activity in the absence of NSC23766, the cells treated with the compound showed a dose-dependent reduction of Rac1-GTP under PDGF stimulation. The presence of 100 μM NSC23766 led to lower than basal level of Rac1-GTP in the cells (Fig. 3*B*). Thus, consistent with the *in vitro* effect on the GEF reaction of Rac1, NSC23766 was able to specifically inhibit Rac1 activation *in vivo*.

PDGF activates Rac1 and induces Rac-mediated membrane ruffles and lamellipodia in fibroblasts (26). To evaluate the ability of NSC23766 to inhibit Rac1-mediated cell functions, we next examined the actin cytoskeleton structures of the cells stimulated by PDGF in the absence or presence of NSC23766. As shown in Fig. 3*C*, 10 nM PDGF potently stimulated membrane ruffling and lamellipodia formation in Swiss 3T3 cells at both 5- and 10-min time lapses. However, in the presence of 50 μM NSC23766, PDGF was only marginally effective in inducing lamellipodia at the cell edges at 5 min and was ineffective at 10 min when control cells that were not treated with NSC23766 displayed significant lamellipodia structures. Essentially all treated cells showed a loss of response to the PDGF stimulation at 10 min with $\approx$70% displaying a complete loss of lamellipodia. These results further indicate that NSC23766 is effective in inhibiting Rac-mediated cellular events.

Inhibition of Serum- or Rac GEF-Induced Cell Growth and Transformation by NSC23766. Rac1 activity is important for cell-growth regulation. Overexpression of dominant negative Rac1 could slow cell growth, whereas constitutively active Rac1 increased the growth rate of fibroblasts (28). Because NSC23766 was able to decrease Rac1 activity in NIH 3T3 cells, we next examined its effect on the growth properties of wild-type NIH 3T3 cells and cells expressing a constitutively active Rac1 mutant, L61Rac1. Comparison of the growth rates of the cells in the absence or presence of 50 μM NSC23766 showed that the compound could slow the growth of wild-type cells without affecting the growth rate of L61Rac1 cells (Fig. 4*A*). The level of GTP-bound L61Racl remained unchanged with or without the compound treatment, whereas the endogenous Rac1 activity in the same cells deceased significantly by NSC23766 (Fig. 4*A*). These results suggest that the inhibitory effect of NSC23766 on cell growth is due to its ability to inhibit cellular Rac1 activity.

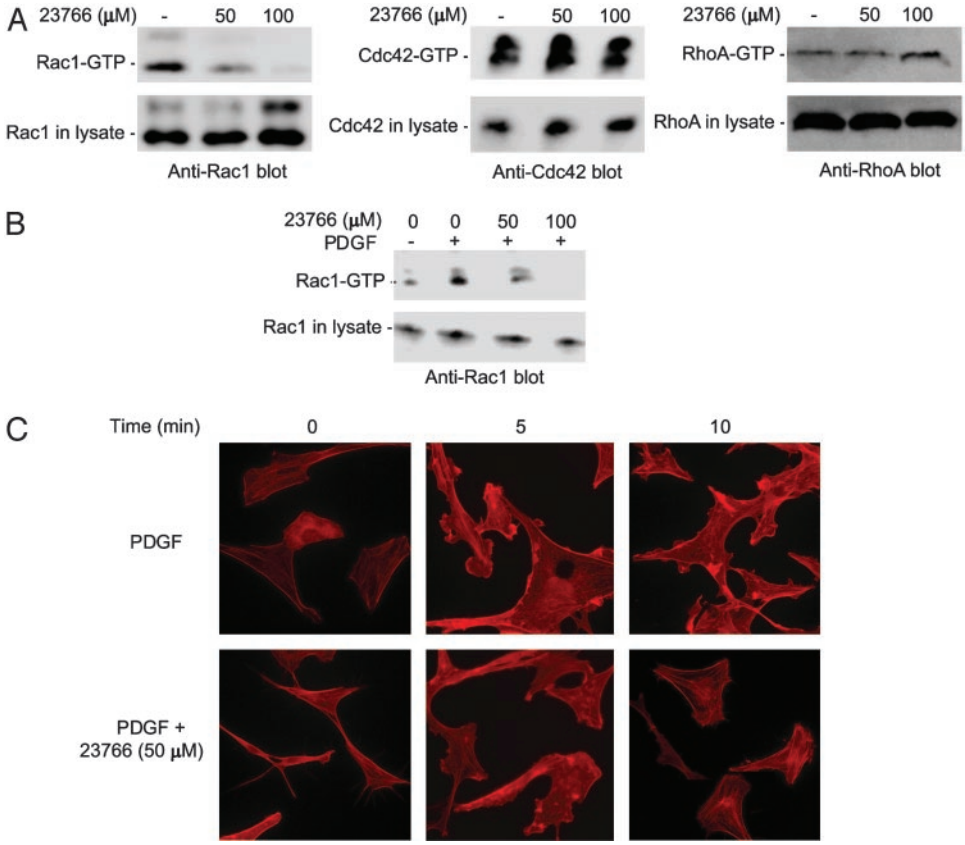

Fig. 3. NSC23766 was effective in specifically inhibiting Rac1 activation in cells. (*A*) The activation states of endogenous Rac1, Cdc42, and RhoA in NIH 3T3 cells with or without NSC23766 treatment were detected by the effector pull-down assays. At 80% confluency in the presence of 10% serum, NIH 3T3 cells in 100-mm dishes were treated with the indicated dosages of NSC23766 for 12 h. Cell lysates containing similar amounts of Rac1, Cdc42, or RhoA were incubated with the agarose-immobilized GST-PAK1, GST-WASP, or GST-Rhotekin, and the co-precipitates were subjected to anti-Rac1, Cdc42 or RhoA Western blot analysis to reveal the amount of GTP-bound Rho proteins. (*B*) The inhibitory effect of NSC23766 on the PDGF-stimulated Rac1 activation was determined by the GST-PAK1 pull-down assay. Serum-starved NIH 3T3 cells in the DMEM with different dosages of NSC23766 were treated with 10 nM PDGF for 2 min. (*C*) NSC23766 inhibited PDGF-stimulated lamellipodia formation. After overnight serum starvation in the presence or absence of 50 μM NSC23766, Swiss 3T3 cells were treated with 10 nM PDGF for the indicated time. The cells were fixed and stained with Rhodamine-labeled phalloidin. Results shown are representative of three independent experiments.

Dbl family GEFs are potent stimulators of cell proliferation because of their ability to directly activate their cognate Rho GTPase substrates. NSC23766 was capable of inhibiting cell growth induced by the Rac1-specific GEF Tiam1 or TrioN (Fig. 4*B* and data not shown), but not that stimulated by the Rho-specific GEF Lbc, the Cdc42-specific GEF Intersectin, or the more promiscuous GEF Vav that acts on Rac with a distinct mechanism (Fig. 4*B* and Fig. 10, which is published as supporting information on the PNAS web site). Moreover, NSC23766 at 50 μM concentration significantly inhibited the foci-forming activity of Tiam1 but not that of L61Rac1 (Fig. 11, which is published as supporting information on the PNAS web site), and it decreased the Tiam1-induced colony numbers and the size of colonies on soft agar (Fig. 4*C*). When applied to the oncogenic Ras (V12H-Ras) transformed cells, NSC23766 partially inhibited the colony-forming activity (Fig. 4*D*). These results further indicate that NSC23766 can act as a specific inhibitory reagent to reverse the cell-proliferative advantage attributed to Rac activation.

Reversal of PC-3 Prostate Tumor Cell Phenotypes by NSC23766. Elevation of Rac1 activity has been associated with cancer cell hyperproliferative and invasive properties. Next, we tested the effect of NSC23766 on the transformation and invasion activities of a prostate cancer cell line, PC-3. PC-3 cells are malignant prostate adenocarcinoma cells derived from the bone metastases of a patient with prostate cancer (29). The mRNA of PTEN tumor suppressor was undetectable in these cells (30), and loss of PTEN has previously been associated with Rac1 hyperactivation because of the significant increase of phosphatidylinositol (3,4,5)-trisphosphate level (31). Indeed, when the activity of endogenous Rac1 in PC-3 cells was examined by probing with GST-PAK1 (p21-binding domain), a significantly higher level of GTP-bound Rac1 than that of normal prostate epithelial cell, RWPE-1, or the relatively indolent LNCaP cells was observed (ref. 32 and data not shown). Inhibition of Rac1 activity in PC-3 cells by expression of either the p21-binding domain of PAK1 or a dominant negative Rac1 mutant could significantly suppress cell growth (ref. 32; data not shown). Thus, we reasoned that the proliferative advantage and other tumor characteristics of PC-3 cells might be mediated by hyperactive Rac1 in the cells, and inhibition of Rac1 activity may reverse some of the traits of PC-3 cells. As shown in Fig. 5 *A* and *B*, treatment of PC-3 cells with NSC23766 led to a dose-dependent inhibition of proliferation and anchorage-independent growth. The size of the colonies of treated cells appeared to be smaller and more compact than those of the untreated ones. Further, at 25 μM, NSC23766 inhibited the PC-3 cell invasion through Matrigel by 85% (Fig. 5*C*). Both PC-3 and RWPE-1 cells remained viable under these conditions. Taken together, these results indicate that NSC23766 was effective in reversing the proliferation, anchorage-independent growth, and invasion phenotypes of PC-3 tumor cells by interfering with Rac activation.

Discussion

Rho family GTPases are important intracellular signaling proteins that control diverse cellular functions related to cancer development, including actin cytoskeleton organization, transcription regulation, cell cycle progression, apoptosis, vesicle trafficking, and cell-to-cell and cell-to-extracellular matrix adhesions (1, 4). They have emerged as potentially useful targets for tumorigenesis (12). In particular, several lines of evidence indicate that the Rho family member, Rac, may play critical roles in several aspects of tumorigenesis and cancer progression. First, constitutively active Rac1 could accelerate cell growth and transform NIH 3T3 cells, whereas dominant negative Rac inhibited cell growth (28). Second, Rac1 was found to be an important component of Ras-induced transformation (3), and the Rac-specific GEF, Tiam1, is involved in Ras-mediated skin cancer progression in mice (33). Third, loss of function in PTEN, p19Arf, or p53 tumor suppressor leads to

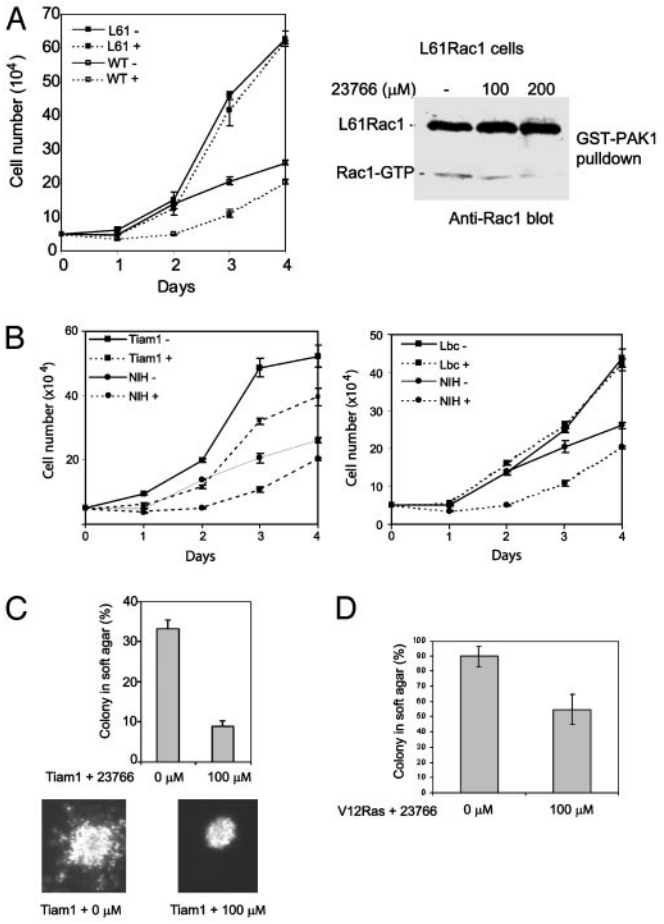

Fig. 4. NSC23766 specifically inhibited Rac GEF-stimulated cell growth and transformation. (*A*) WT or L61Rac1-expressing NIH 3T3 cells were grown in 5% serum in the presence (– – –) or absence (—) of 100 μM NSC23766. The cells were split in triplicate in six-well plates at a density of 5×10^4 cells per well. The GTP-bound L61Rac1 and endogenous Rac1 of the L61Rac1-expressing cells were probed by GST-PAK1 pull-down after 12 h treatment with increasing concentrations of NSC23766. (*B*) WT or the GEF (Tiam1 or Lbc)-expressing NIH 3T3 cells were grown in 5% serum in the presence (– – –) or absence (—) of 100 μM NSC23766, and the cell numbers were determined by daily cell counting. (*C*) Stable transfectant of Tiam1-expressing NIH 3T3 cells were cultured in 0.3% soft-agar medium for 14 days in the presence or absence of 100 μM NSC23766. The number and the morphology of the colonies were examined under a microscope. (*D*) Stable V12-H-Ras-expressing NIH 3T3 cells were assayed for the growth in the soft-agar medium in the presence or absence of 100 μM NSC23766. The colonies were scored 14 days after plating.

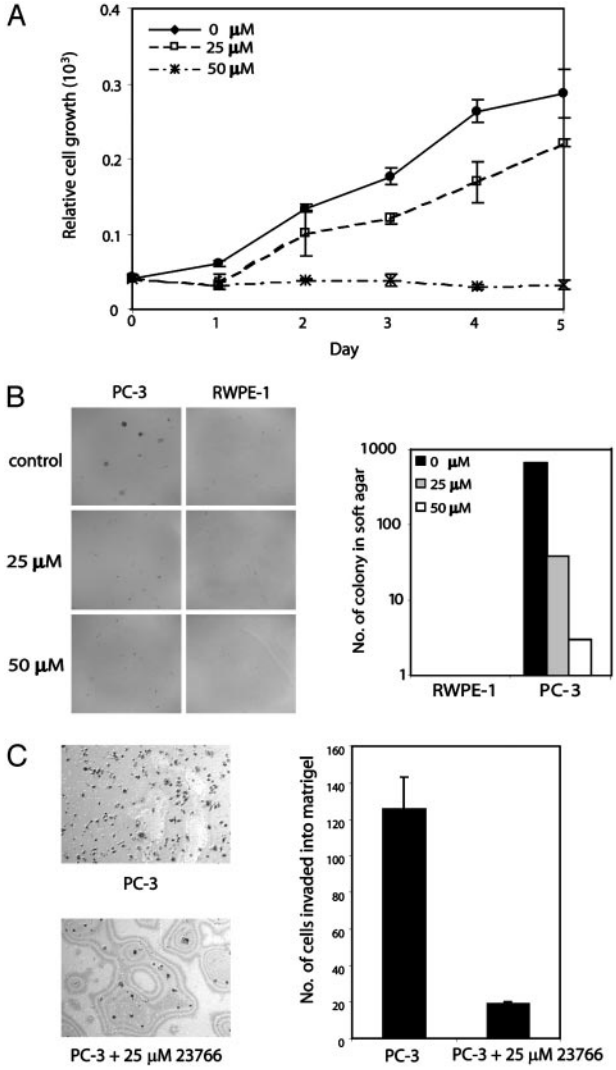

Fig. 5. NSC23766 inhibited the proliferation, anchorage-independent growth and invasion of PC-3 prostate cancer cells. (*A*) PC-3 cells were grown in 5% calf serum supplemented with the indicated concentrations of NSC23766. The cells were split in triplicate in 96 wells at 1.5×10^3 cells per well. Cell numbers were assayed by using CellTiter 96 AQueous cell proliferation assay kit in different days. (*B*) PC-3 and RWPE-1 prostate epithelial cells (1.25×10^3 per well) were grown in 0.3% agarose in different doses of NSC23766, and the number of colonies formed in soft agar was quantified 12 days after plating. (*C*) PC-3 cells were placed in an invasion chamber for 24 h at 37°C in the absence or presence of 25 μM NSC23766.

elevation of Rac activity, resulting increased migration and proliferation in *PTEN*$^{-/-}$, *p19Arf*$^{-/-}$, or *p53*$^{-/-}$ cells (31, 34, 35). Fourth, hyperactive Rac1 and Rac3 were associated with the increased proliferation of several breast cancer cell lines (8, 10). In addition, a point mutation of Tiam1 has been identified in human tumors, and this mutant was shown to transform NIH 3T3 cells (36). Unlike Ras, however, constitutively active mutation of Rac has not been found in human cancer. It is possible that up-regulation or overexpression, rather than GTPase-defective mutation, of Rac is associated with tumorigenic properties. Therefore, the signaling step of Rac1 activation by GEF could be a targeting site of the signaling chains involving Rac.

In previous work we have demonstrated that Trp^{56} of Rac1 is the critical structural determinant specifying Rac1 recognition and responsiveness to a subset of Rac-specific GEFs (16). A peptide derived from Rac1 sequences, including the Trp^{56} residue, was able to block the interaction between Rac and several of Rac-specific GEFs without affecting the effector PAK1 binding. We speculated that the structural features of Rac1 in the region containing Trp^{56} could be explored to design inhibitors to specifically interfere with Rac1 activation by GEFs. In the present study, based on the structural information provided by the Rac1–Tiam1 complex and by taking the computer-simulated virtual screening approach, we have identified the small chemical compound of the National Cancer Institute chemical database, NSC23766, as a Rac-specific inhibitor. We show that this compound was able to discriminate Rac1 from Cdc42 and RhoA and specifically inhibited Rac1 activation by its GEF *in vitro* and *in vivo*. We provide an example of application of this compound to a human cancer cell line, PC-3, and show that it was able to inhibit proliferation, anchorage-independent growth, and invasion of the Rac-hyperactive prostate cancer cells by down-regulating the endogenous Rac1 activity.

To understand the inhibitory mechanism of NSC23766 on Rac1, we examined the simulated model of NSC23766 docking on Rac1

(Fig. 1*B*). In the model, the binding site for NSC23766 in Rac1 is a surface cleft formed by residues Lys^5, Val^7, Asp^{38}, Asn^{39}, Trp^{56}, Asp^{57}, Thr^{58}, Leu^{70}, and Ser^{71}. The major bonding involved in the interaction between NSC23766 and Rac1 is hydrophobic in nature. The nitrogen atoms of NSC23766 form three hydrogen bonds with residues from the backbone of Rac1, and the stacking effect of the middle pyrimidine ring of NSC23766 with the indole ring of Trp^{56} may also contribute significantly to the interaction. We suspect that the interaction between Trp^{56} and the aromatic ring of NSC23766 governs the binding specificity of 23766, and the selectivity of Rac1 over Cdc42 by NSC23766 might be because the side chain of Trp^{56} in Rac1 provides sufficient bonding for the recognition of NSC23766, whereas the smaller side chain of Phe^{56} in Cdc42 fails to establish a relatively high-affinity interaction with NSC23766. Moreover, the binding pocket of NSC23766 in Rac1 is located at the three-way junction site of switch I, switch II, and $\beta1/\beta2/\beta3$, where it provides much of the binding surface for Tiam1 recognition in the Rac1–Tiam1 crystal structure (13). It is possible that NSC23766 may not only interfere with the interaction between $\beta1/\beta2/\beta3$ of Rac1 and Tiam1, but also inhibit the interaction of the switch regions with Tiam1. Such a docking model is supported by the Rac1 mutant results (Fig. 1*C*) and our preliminary NMR ^{15}N-heteronuclear sequential quantum correlation chemical-shift perturbation data obtained by titrating NSC23766 to the N^{15}-labeled Rac1. Thus, the strategic localization of the binding pocket could be the reason that NSC23766 is able to efficiently inhibit the activation of Rac1 by Trio or Tiam-1, and the specific binding of NSC23766 to Rac1 may involve the overall conformation of Trp^{56} and its neighboring residues.

As a first generation inhibitor for Rac, NSC23766 is capable of specifically interfering with Rac1 but with not Cdc42 or RhoA activation by their respective GEFs, as demonstrated by the *in vitro* binding and exchange assays (Figs. 2 and 9) and the *in vivo* Rho GTPase effector domain pull-down assays (Fig. 3). The compound could further affect the downstream signaling events of Rac, such as membrane ruffling and lamellipodia formation induced by upstream stimulus PDGF (Fig. 3). Consistent with its role as a competitive inhibitor of Rac activation, the effects of the compound on Rac1 activity and Rac-mediated cellular function appear to be reversible, because medium changes of the cells treated with NSC23766 could diminish the Rac-inhibitory effect (Y.G. and Y.Z., unpublished data). Although we cannot rule out the possibility that NSC23766 has additional targets *in vivo*, the facts (*i*) that it can specifically block cell growth stimulated by the Rac1-specific Trio and Tiam1, but not that caused by the RhoA or Cdc42-specific Lbc and Intersectin, or by the more promiscuous Rho GTPase GEF Vav that utilizes a distinct mechanism to couple to Rac (37, 38) and (*ii*) that it inhibited the cell growth stimulated by serum but not by that induced by the constitutively active L61Rac1 strongly suggest that NSC23766 may work specifically through interference of Rac1 activation to elicit its inhibitory effect on cells.

The data we gathered of NSC23766 in fibroblast cells suggest that it might have antioncogenic potential in tumor cells. To demonstrate that NSC23766 might be useful to reverse tumor cell phenotypes, we examined the prostate cancer PC-3 cells that depend on hyperactive Rac1 activity for growth and invasion properties (32), possibly because of the impairment of PTEN expression in these cells (30). Application of NSC23766 to PC-3 cells resulted in significant inhibition of proliferation, anchorage-independent growth, and invasion, indicating that interfering with Rac activation by NSC23766 is an encouraging approach for tumor cell repression. The results of this preliminary study open the door for further testing of this chemical in other tumor cell types in which Rac signaling is deregulated. In addition to the effect on cell growth and invasion, we noticed that NSC23766 was able to cause cell rounding and detachment from the matrix (Y.G. and Y.Z., unpublished data), possibly affecting cell adhesion mediated by Rac1 (39). We also noticed a difference in dose dependence between PC-3 cells and fibroblasts, which might reflect the difference in cell types in uptaking efficiency or dependence on Rac1 activity. A more detailed examination of the efficacy of the compound in various cell types is warranted to determine the optimal dose required for each cell system.

To further improve the inhibitory effect of NSC23766 on Rac1 activation, we must attempt to modify the structure of NSC23766 to achieve a better fitting into the groove on the Rac1 surface and to increase the docking affinity. Recently, a small-molecule compound and its derivatives were discovered as inhibitors of Ras–Raf interaction by a forward two-hybrid screening (40). These compounds could reverse the transformation phenotypes induced by Ras in several cancer cell lines at a concentration of $\approx 20\ \mu M$. Rac acts further downstream of Ras and contributes to Ras transformation. NSC23766 can partially inhibit oncogenic Ras-induced cell transformation, raising an attractive possibility that it might work synergistically with the Ras–Raf interaction inhibitors to effectively reverse Ras-mediated tumorigenesis because Rac1 and Raf are involved in different aspects of Ras-mediated growth regulation (3).

We thank Dr. Channing Der (University of North Carolina, Chapel Hill) for providing a Tiam1 construct and Dr. J. Silvio Gutkind (National Institutes of Health, Bethesda) for a PDZ-RhoGEF construct. This work was supported by National Institutes of Health Grants GM60523 and GM53943 (to Y.Z.) and GM61739 (to J.Z.).

1. Etienne-Manneville, S. & Hall, A. (2002) *Nature* **420,** 629–635.
2. Zheng, Y. (2001) *Trends Biochem. Sci.* **26,** 724–732.
3. Zohn, I. M., Campbell, S. L., Khosravi-Far, R., Rossman, K. L. & Der, C. J. (1998) *Oncogene* **17,** 1415–1438.
4. Van Aelst, L. & D'Souza-Schorey, C. (1997) *Genes Dev.* **11,** 2295–2322.
5. Schmitz, A. A., Govek, E. E., Bottner, B. & Van Aelst, L. (2000) *Exp. Cell Res.* **261,** 1–12.
6. Symons, M. (2000) *Curr. Biol.* **10,** R535–R537.
7. Fritz, G., Just, I. & Kaina, B. (1999) *Int. J. Cancer* **81,** 682–687.
8. Mira, J. P., Benard, V., Groffen, J., Sanders, L. C. & Knaus, U. G. (2000) *Proc. Natl. Acad. Sci. USA* **97,** 185–189.
9. Kamai, T., Arai, K., Tsujii, T., Honda, M. & Yoshida, K. (2001) *BJU Int.* **87,** 227–231.
10. Schnelzer, A., Prechtel, D., Knaus, U., Dehne, K., Gerhard, M., Graeff, H., Harbeck, N., Schmitt, M. & Lengyel, E. (2000) *Oncogene* **19,** 3013–3020.
11. Suwa, H., Ohshio, G., Imamura, T., Watanabe, G., Arii, S., Imamura, M., Narumiya, S., Hiai, H. & Fukumoto, M. (1998) *Br. J. Cancer* **77,** 147–152.
12. Sahai, E. & Marshall, C. (2002) *Nat. Rev. Cancer* **2,** 133–142.
13. Worthylake, D. K., Rossman, K. L. & Sondek, J. (2000) *Nature* **408,** 682–688.
14. Rossman, K. L., Worthylake, D. K., Snyder, J. T., Siderovski, D. P., Campbell, S. L. & Sondek, J. (2002) *EMBO J.* **21,** 1315–1326.
15. Snyder, J. T., Worthylake, D. K., Rossman, K. L., Betts, L., Pruitt, W. M., Siderovski, D. P., Der, C. D. & Sondek, J. (2002) *Nat. Struct. Biol.* **9,** 468–475.
16. Gao, Y., Xing, J., Streuli, M., Leto, T. L. & Zheng, Y. (2001) *J. Biol. Chem.* **276,** 47530–47541.
17. Karnoub, A. E., Worthylake, D. K., Rossman, K. L., Pruitt, W. M., Campbell, S. L., Sondek, J. & Der, C. J. (2001) *Nat. Struct. Biol.* **8,** 1037–1041.
18. Waszkowycz, B., Perkins, T. D. J., Sykes, R. A. & Li, J. (2001) *IBM Systems J.* **40,** 360–376.
19. Gruneberg, S., Wendt, B. & Klebe, G. (2001) *Angew. Chem. Int. Ed. Engl.* **40,** 389–393.
20. Zhang, B., Zhang, Y., Wang, Z. & Zheng, Y. (2000) *J. Biol. Chem.* **275,** 25299–25307.
21. Qiu, R. G., Abo, A., McCormick, F. & Symons, M. (1997) *Mol. Cell. Biol.* **17,** 3449–3458.
22. Wang, L., Yang, L., Luo, Y. & Zheng, Y. (2003) *J. Biol. Chem.* **278,** 44617–44625.
23. Hurst, T. (1994) *J. Chem. Inf. Comput. Sci.* **34,** 190–196.
24. Rarey, M., Kramer, B., Lengauer, T. & Klebe, G. (1996) *J. Mol. Biol.* **261,** 470–489.
25. Clark, R. D., Strizhev, A., Leonard, J. M., Blake, J. F. & Matthew, J. B. (2002) *J. Mol. Graphics Model* **20,** 281–295.
26. Ridley, A. J., Paterson, H. F., Johnston, C. L., Diekmann, D. & Hall, A. (1992) *Cell* **70,** 401–410.
27. Hawkins, P. T., Eguinoa, A., Qiu, R. G., Stokoe, D., Cooke, F. T., Walters, R., Wennstrom, S., Claesson-Welsh, L., Evans, T., Symons, M. & Stephens, L. (1995) *Curr. Biol.* **5,** 393–403.
28. Khosravi-Far, R., Solski, P. A., Clark, G. J., Kinch, M. S. & Der, C. J. (1995) *Mol. Cell. Biol.* **15,** 6443–6453.
29. Kaighn, M. E., Narayan, K. S., Ohnuki, Y., Lechner, J. F. & Jones, L. W. (1979) *Invest. Urol.* **17,** 16–23.
30. Bastola, D. R., Pahwa, G. S., Lin, M. F. & Cheng, P. W. (2002) *Mol. Cell Biochem.* **236,** 75–81.
31. Liliental, J., Moon, S. Y., Lesche, R., Mamillapalli, R., Li, D., Zheng, Y., Sun, H. & Wu, H. (2000) *Curr. Biol.* **10,** 401–404.
32. Lyons, L. S., Krajewski, S. K., Welsh, C. & Burnstein, K. L. (2003) *Proc. Am. Assoc. Cancer Res.* **44,** 273 (R1404).
33. Malliri, A., van der Kammen, R. A., Clark, K., van der Valk, M., Michiels, F. & Collard, J. G. (2002) *Nature* **417,** 867–871.
34. Guo, F., Gao, Y., Wang, L. & Zheng, Y. (2003) *J. Biol. Chem.* **278,** 14414–14419.
35. Guo, F. & Zheng, Y. (2003) *Mol. Cell. Biol.* **24,** 1426–1428.
36. Engers, R., Zwaka, T. P., Gohr, L., Weber, A., Gerharz, C. D. & Gabbert, H. E. (2000) *Int. J. Cancer* **88,** 369–376.
37. Olson, M. F., Pasteris, N. G., Gorski, J. L. & Hall, A. (1996) *Curr. Biol.* **6,** 1628–1633.
38. Movilla, N., Dosil, M., Zheng, Y. & Bustelo, X. R. (2001) *Oncogene* **20,** 8057–8065.
39. Del Pozo, M. A., Price, L. S., Alderson, N. B., Ren, X. D. & Schwartz, M. A. (2000) *EMBO J.* **19,** 2008–2014.
40. Kato-Stankiewicz, J., Hakimi, I., Zhi, G., Zhang, J., Serebriiskii, I., Guo, L., Edamatsu, H., Koike, H., Menon, S., Eckl, R., *et al.* (2002) *Proc. Natl. Acad. Sci. USA* **99,** 14398–13303.